Streptococcus bovis JB1 Protects Against Oxidative Stress Caused by *comC* Knockout by Increasing Trehalose Secretion

Quanhui Peng[1]*, Ali Mujtaba Shah[2]*, Wang Zhi-Sheng[1], Xue Bai[1], Wang Li-Zhi[1], Zou Hua-Wei[1], Ali Raza Shah[3], Jiang Ya-Hui[1], Hu Rui[1] and Xiao Jian-Xing[1]

[1]*Institute of Animal Nutrition, Key Laboratory of Bovine Low-Carbon Farming and Safe Production, Sichuan Agricultural University, Chengdu, 611130, PR China*

[2]*Key Laboratory of Animal Genetics, Breeding and Reproduction of Shaanxi Province, College of Animal Science and Technology, Northwest A and F University, Yangling 712100, China.*

[3]*Khairpur College of Agricultural Engineering and Technology, Sindh Agriculture University, Tandojam, 66000, Sindh, Pakistan*

Quanhui Peng and Ali Mujtaba Shah contributed equally to this work.

ABSTRACT

Streptococcus bovis mainly produces lactic acid in the rumen leading to acute rumen acidosis, and can also cause diseases such as infective endocarditis and colorectal cancer. The growth and reproduction of *S. bovis* mainly relies on ComC and ComDE, a quorum sensing system. In this study, a *comC* knockout model was constructed (*ΔcomC* mutant), and metabolomics was applied to investigate its effect on cell metabolism. The growth rate of *ΔcomC* mutant decreased, and the results of PCA and PLS-DA analysis showed that the intracellular metabolites could be completely separated from the wild type, among which the trehalose increased by 96 times, glucose and mannitol, etc. increased by 4 times, and putrescine and 2-Hydroxyglutaric acid increased by 2 times, whereas the valine, leucine, isoleucine, proline and cysteine etc. were dramatically reduced. Analyses of KEGG showed phenylalanine metabolism, pyruvate metabolism, glyoxylate and dicarboxylate metabolism as enriched pathways. In conclusion, *S. bovis* promotes energy metabolism and secrets huge amounts of trehalose and mannitol to form biofilm to resists oxidative stress caused by *comC* knockout. The synthetic pathway of trehalose can be used as a drug target for the prevention or treatment of *S. bovis*.

INTRODUCTION

A *Streptococcus bovis/Streptococcus equinus* complex (SBSEC) of domesticated animals, particularly cows and horses, is a non-enterococcal group D *Streptococcus* spp. complex. It is composed of 7 (sub) species. For example, *S. bovis* can cause acute ruminal acidosis and bloat in cows and is often associated with mastitis. (Pompilio and Di Bonaventura, 2019). In spite of the lack of

*　　　Corresponding author: pengquanhui@126.com, alimujtabashah@nwafu.edu.cn

precise numbers, it is generally recognized that SBSEC infection of cattle results in significant losses, nearly a billion dollars annually (Herrera *et al*., 2009). As an emerging pathogen that causes infectious endocarditis in humans and is strongly associated with colorectal cancer, SBSEC is receiving increasing attention from scientists (Kaiki *et al*., 2021; Öberg and Nilson, 2022).

S. mutans has a quorum sensing (QS) system that consists primarily of a signal peptide and the ComDE two-component regulatory system. Its QS signal is a 21-amino-acid peptide pheromone called the competence stimulating peptide (CSP) (Asanuma *et al*. 2010). In the extracellular environment, this peptide accumulates from CSP precursors (encoded by *comC*). CSP stimulates the sensor histidine kinase (ComD) and the response regulator (ComE) when its concentration reaches a critical threshold (Suntharalingam and Cvitkovitch, 2005). It has been found that the CSP-dependent QS system regulates a variety of physiological activities in S mutans, including bacteriocin productions, competence development, formation of

biofilms, and stress response (OmerOglou *et al*., 2022).

Yang and Tal-Gan (2019) revealed developing novel streptococcus QS modulators with higher potency and improved pharmacological properties has been possible by identifying structural features that are optimal to achieve receptor ComD activation and understanding the CSP:ComD interaction. New generations of antibacterial agents may be able to treat Streptococcus diseases by modulating Streptococcus QS through intercepting CSP: ComD interactions. Based on this advancement, it is reported that 7S globulin 3 derived from the adzuki bean (Senpuku *et al*., 2019), sodium new houttuyfonate (Shui *et al*., 2019) and fructanase (Suzuki *et al*., 2017) had inhibiting effects on competence-stimulating peptide-dependent QS system in *S. mutans*. The deletion of entire comC and two-thirds of comD reduced growth rate, which may be related to changes in protein expression (Asanuma *et al*., 2004). However, the effect of *comC* deletion on the metabolism of the cells has not been elucidated till now.

Therefore, the objectives of the present study were to investigate the metabolic changes operating in *comC* knockout *Sreptococcus bovis* JB1 strain by employing metabolomics. The results of this study will contribute to a comprehensive and in-depth understanding of QS regulatory mechanism, and possibly provide preventative methods for tackling *S. bovis* biofilms.

MATERIALS AND METHODS

Sources of Streptococcus bovis *and culture conditions*

The *S. bovis* JB1 was screened from a native beef cattle (Xuanhan Yellow Cattle) and identified previously by our team. The diet given in Supplementary Table S1 was presented to the cattle. *S. bovis* was chronically grown in our laboratory. Briefly, the medium contained (g/L): casein peptone, 10.0; beef extract 10.0; yeast extract, 5.0; glucose, 5.0; sodium acetate, 2.0; Tween 80, 1.0; K_2HPO_4, 2.0; $MgSO_4 \cdot 7H_2O$, 0.2; $MgSO_4 \cdot H_2O$, 0.05; $CaCO_3$, 20.0; agar, 15.0. The pH of culture incubations was maintained between 6.8~7.0.

Construction of a comC-*disrupted mutant of* S. bovis

A *comC*-disrupted mutant (ΔcomC) was constructed as described previously *BY* Asanuma *et al*. (2004). The upper and lower regions of *comC* were amplified by PCR and blunt ended by T4 DNA polymerase (TaKaRa, Dalian, China). With the help of DNA ligase T4 (TaKaRa, Dalian, China), *ermB*, the erythromycin resistance gene, was inserted between the upper and down regions of comC. The plasmid pUC18 (TaKaRa, Dalian, China) was used as the carrier of ligated product. Using an electroporated plasmid, the recombinant plasmid was transferred to *S. bovis* strain JB1. Transformants were finally selected with erythromycin

(10 μg/mL). All restriction enzymes and T4 DNA ligase were obtained from Takara Biotechnology (Dalian, China).

Quantification of metabolome changes using GC-MS

Harvested cells were at the mid-exponential phase (OD_{600}=0.7). The pre-treatment method of microbiology was defined by (Smart *et al*., 2010). A gas chromatography-mass spectrometry (GC–MS) apparatus was used with 1 μL samples (with Inert MSD: 7890A, 5975C, 7693 autosamplers) with a phenylmethylsilicone 5% capillary column, 30m×0.250mm×0.25μm. With the injector set to 280°C, splitless injection was performed. The column oven temperature was programmed at 70°C for 2 min, then 30°C at 10°C/min for 5 min. Five ions were monitored for each analyte by electronic energy 70 ev identification: 73, 101, 148, 203, 204 for levamisole, 56, 91, 118, 145, and 162 for aminorex, 73, 91, 162, 291, and 306 for bis-trimethylsilyl aminorex, and 72, 148, and 91 for mephentermine. Analyses were also performed in scan mode under the same chromatographic conditions.

Statistical analysis

An analysis of multivariate data was performed in accordance with Qiu *et al*. (2016). Simca-P1 v 12.0 (Umetrics, Sweden) was used to validate the models using a seven-fold cross-validation method using the partial least square discriminant (PLS-DA) with Unit Variance scaling. Using CV-ANOVA, the significance of the PLS-DA model was verified. We assessed the importance of each metabolite in the PLS-DA based on variable importance in projections (VIP).

RESULTS

Growth curves of Streptococcus bovis *JB1 and* ΔcomC *mutant*

The growth of *S. bovis* was monitored via measuring the optical density at 600 nm (OD_{600}). *S. bovis* was harvested till the late exponential growth phase. The OD value of *ΔcomC* mutant (KO) at growth cessation was lower than that of the wild type (WT). The *ΔcomC* mutant reach the growth plateau was about 30 min later than the wild type (Fig. 1). Subsequently, the bacterial cells were harvested and metabolomic tool was applied, and LC/MS (Agilent 7890A) platform were used in determining the intracellular metabolites.

Classification of annotated metabolites

Through the detection, the total ion chromatogram (TIC) of each group of typical samples is shown in Supplementary Fig. S1. From the total ion chromatogram, the samples of the two groups were different. A total of 140 peaks were detected, however according to existing

databases and standards, of which only a total of 78 substances were annotated, the details can be seen in supplementary material "Metabolome.xlsx". These substances were mainly primary metabolites, the specific classification as shown in Supplementary Figure S2.
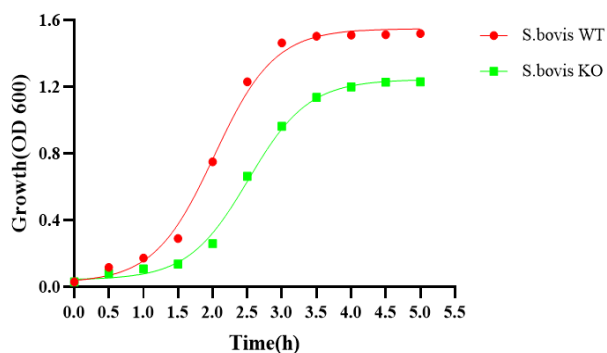

Fig. 1. Growth curves of *Sreptococcus bovis* JB1 wild type (WT) and *ΔcomC* mutant (KO).

Principal component analysis (PCA)

The PCA scores plot of the two groups was presented in Figure 2A. All of the sample plots were in Hotelling T2 ellipse (95%). The KO group could be clearly distinguished from WT group. Two principal components were obtained, and the parameters of the model for the two groups was R2X=0.756, Q2=0.546. In addition, supervised clustering method PLS-DA was also used to classify the two groups. Model was established for the first and second principal components after unit variable scaling was applied. We can see that the clustering result was similar with PCA scores plot (Fig. 2B). The KO group can be clearly differentiated with WT group. The model was tested by leave-one-out cross validation, and the model cumulative explanation rate parameters was R2Y=0.997, Q2=0.973. The R2Y=0.997 meant the fit goodness of the model was high, and the Q2=0.973 meant the predictive ability of the model was strong. Permutation test result indicated that the intercept of R2 on the Y axis was 0.613 and the intercept of Q2 on the Y axis was -0.0424. This meant that the model did not have excessive fitting (Fig. 2C).

Variable importance in projections (VIP)

Figure 3 shows a VIP plot of the PLS-DA of the KO and WT groups, in which the metabolites were ranked according to their importance in discriminating KO and WT. Using VIP plots, the top 15 important metabolites were shown. A higher VIP value indicates a greater contribution to the difference between WT and KO. The VIP plots indicated that trehalose, proline, 2-hydroxyglutaric acid, valine, leucine, isoleucine, tyramine, 1, 3-Di-tert-

butylbenzene, putrescine, oxalic acid, glycine, heptanoic acid, pipecolic acid, aspartic acid and ornithine were the strongest discriminating metabolites for separating KO and WT group. The heatmap on the right side of the VIP plots indicated that 8 (i.e., trehalose, 2-hydroxyglutaric acid, tyramine, 1,3-Di-tert-butylbenzene, putrescine, oxalic acid, glycine and aspartic acid) out of 15 metabolites were increased while 7 metabolites (proline, valine, leucine, isoleucine, heptanoic acid, pipecolic acid and ornithine) were decreased.
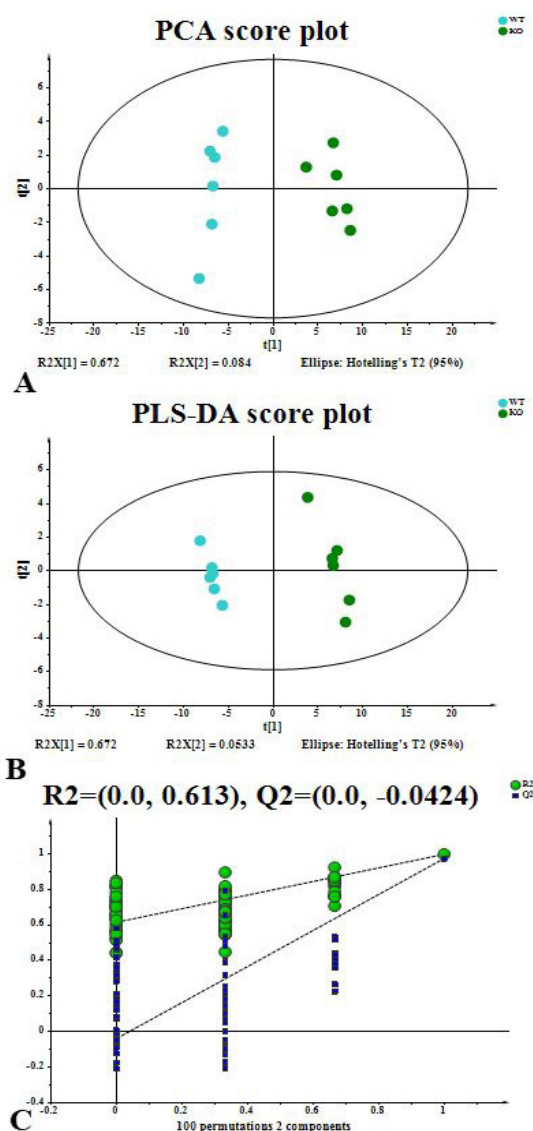

Fig. 2. Principal components analysis (PCA)(A), partial least squares discriminant analysis (PLS-DA)(B) and permutation test result of PLS-DA (C). Blue circle is *Sreptococcus bovis* JB1 wild type (WT), and green circle is *ΔcomC* mutant (KO).

Pathways

The top 6 affected pathways of KO group compared with wild type were glyoxylate and dicarboxylate metabolism, alanine, aspartate and glutamate metabolism, pyruvate metabolism, cysteine and methionine metabolism, glutathione metabolism, arginine and proline metabolism (Table II, Fig. 4). The alteration of pathways was caused by the change of metabolites reflected in Table I.
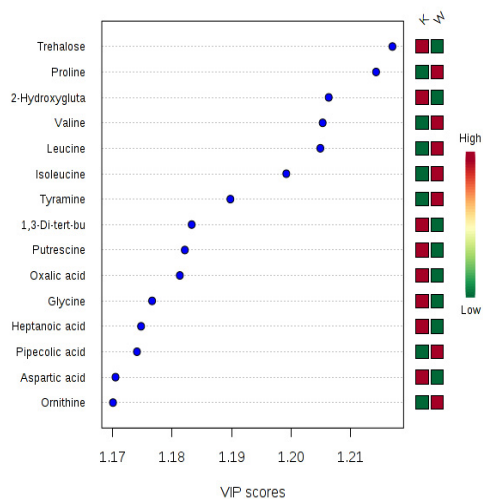

Fig. 3. Important features of differently expressed metabolites obtained from *Sreptococcus bovis* JB1 wild type (WT) and *ΔcomC* mutant (KO) identified by partial least squares discriminant analysis (PLS-DA). The colored boxes on the right indicate the relative concentrations of the corresponding metabolites in each group under study.
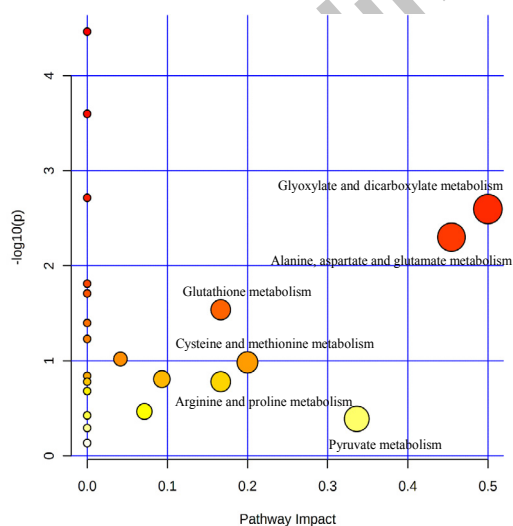

Fig. 4. Metabolome view map of the differentially expressed metabolites obtained from *Sreptococcus bovis* JB1 wild type and *ΔcomC* mutant.

Table I. Different expressed metabolites of intracellular content of *Sreptococcus bovis* JB1 wild type (WT) and *ΔcomC* mutant (KO).

No.	Compounds	KO vs. WT	
		FC	P-value
1	Trehalose	96.313	<0.001
2	Mannitol	4.927	<0.001
3	Glucose	4.163	<0.001
4	Monomethylphosphate	4.072	<0.001
5	Sucrose	3.941	0.003
6	Glycolic acid	3.922	0.004
7	Glycine	3.686	<0.001
8	Hydroxylamine	2.829	<0.001
9	Nonadecanoic acid	2.729	<0.001
10	Putrescine	2.591	<0.001
11	2-Hydroxyglutaric acid	2.586	<0.001
12	Oxalic acid	2.581	<0.001
13	Urea	2.502	0.028
14	1,3-Di-tert-butylbenzene	2.485	<0.001
15	2,4,6-Tri-tert.-butylbenzenethiol	2.459	<0.001
16	Serine	2.435	<0.001
17	Citric acid	2.416	<0.001
18	Heptanoic acid	2.409	<0.001
19	Pyruvic acid	2.391	<0.001
20	Dodecanoic acid	2.349	<0.001
21	Asparagine	2.349	<0.001
22	Hexadecanol	2.325	<0.001
23	Benzoic acid	2.206	<0.001
24	Ribose	2.079	0.003
25	Octadecanol	2.070	<0.001
26	Nonanoic acid	2.034	<0.001
27	Pipecolic acid	0.499	<0.001
28	Valine	0.403	<0.001
29	Isoleucine	0.344	<0.001
30	9-Z-Octadecenoic acid	0.326	0.020
31	Leucine	0.308	<0.001
32	9-Z-Hexadecenoic acid	0.296	0.018
33	Cysteine	0.243	<0.001
34	Glutamine	0.235	<0.001
35	Ornithine	0.234	<0.001
36	Tyramine	0.199	<0.001
37	Proline	0.181	<0.001

All different metabolites listed here are those VIP>1, fold change >2 or <0.5 and *P* value<0.05.

Table II. Significant different metabolites that enriched in the pathways of intracellular content obtained from *Sreptococcus bovis* JB1 wild type and *ΔcomC* mutant.

Pathway	Total Cmpd	Hits	Raw p	-log (p)	Holm adjust	FDR p	Impact
Glyoxylate and dicarboxylate metabolism	15	3	1.52E-04	8.79E+00	2.13E-03	2.10E-04	0.50
Alanine, aspartate and glutamate metabolism	18	7	3.26E-10	2.18E+01	1.43E-08	3.82E-09	0.45
Pyruvate metabolism	20	3	3.32E-04	8.01E+00	4.32E-03	4.46E-04	0.34
Cysteine and methionine metabolism	25	6	5.77E-10	2.13E+01	2.48E-08	5.42E-09	0.20
Glutathione metabolism	13	3	2.67E-10	2.20E+01	1.22E-08	3.82E-09	0.17
Arginine and proline metabolism	30	8	9.02E-09	1.85E+01	3.43E-07	4.24E-08	0.17

DISCUSSION

The glycosidic bond between two molecules of glucose makes trehalose a non-reducing disaccharide. As a typical stress metabolite, trehalose can form a protective film on cell surfaces when exposed to harsh environmental conditions, including high temperature, high cold, high osmotic pressure, drying, and water loss. In this way, the biomolecular structure is effectively protected from destruction, and the living body's life process and biological characteristics are preserved (Câmara *et al*., 2019; Izanloo *et al*., 2021; Kokina *et al*., 2022; Wei *et al*., 2022). Câmara *et al*. (2019) reported that cells naturally enriched in trehalose or glutathione acquired resistance to dehydration, preventing the oxidation of glutathione. In this study, the concentration of trehalose in the *ΔcomC* mutant was increased by 96-fold, which was the most surprising finding of this study. This verified that trehalose was indeed a stress metabolite. Our KEGG result showed that the glutathione pathway was also significantly enriched. The reduced glutathione form is metabolized in multiple ways, leading to glutamate, cysteine, and glycine biosynthesis (Koga *et al*., 2011), therefore the concentration of glycine and cysteine, and the glutamate metabolism pathway was changed in the *ΔcomC* mutant when compared with the wild type. Bacteria alter growth and biofilm formation in the face of stress, and biofilm is the way of bacteria to resist stress (Peterson *et al*., 2015). Polysaccharides, lipids, adhesive proteins, and secreted extracellular DNA make up the biofilm matrix (Hobley *et al*., 2015). In this experiment, we observed a 4-fold increase in mannitol concentration under of *comC* knockout stress conditions. The mechanism of mannitol production has been elaborated in previous studies (Hu *et al*., 2018). Taken together, under the condition of *comC* knockout stress, the synthesis and secretion of trehalose and mannitol were increased.

A 4-fold increase in glucose concentration was observed in our study, and previous studies have shown that *E. coli* could enhance its tolerance by using exogenous glucose under conditions of ofloxacin stress. When glucose was consumed, its growth rate decreased (Amato *et al*., 2013). In addition, the glyoxylate and dicarboxylate metabolism plays a very important role in the energy metabolism in many fungi as a bypass for the tricarboxylic acid cycle (Padilla-Guerrero *et al*., 2011). The enriched glyoxylate and dicarboxylate metabolism pathway may help producing more glucose. Therefore, high glucose production and utilization may be one of the mechanisms by which *S. bovis* resist various stress.

Usually, amino acids are decomposed by decarboxylation groups to form various amines. For example, glycine, ornithine, arginine, histidine and tyrosine are degraded to form methylamine, putrescine, histamine, tyramine and other putrefactive amines, which are toxic to the biological environment (de las Rivas *et al*., 2006; Henao-Escobar *et al*., 2015). In this experiment, the concentration of hydroxylamine, putrescine, tyramine was changed when the *comC* was knockout. The putrescine produced by bacteria are mainly via ornithine decarboxylase or agmatine deiminase pathway (Ahmad *et al*., 2020), which was attributed to the decrease of ornithine. It is reported that 2-hydroxyglutaric acid bind and inhibit ATP synthase and mTOR signaling and showed a growth-suppressive function (Fu *et al*., 2015). The 2-fold increase of 2-hydroxyglutaric acid accounted for the decreased growth of *ΔcomC* mutant observed in this study. Pyruvate was reported to enable the proliferation of RC-deficient cells and increased the content of aspartate (Chen *et al*., 2016), which was in agreement with our study. The enriched pyruvate metabolism pathway in our study may be a compensatory mechanism for inhibited cell growth.

The branched amino acids were all decreased when the *comC* was knockout. The amount of amino acids (valine, leucine, isoleucine, threonine, arginine, glutamate, phenylalanine) decreased significantly when sea cucumber,

Apostichopus japonicus facing high temperature stress (above 25 °C) (Shao *et al.*, 2015), and the metabolomic profiles of budding yeast cells were consistent with these observations: pyruvic acid accumulation, TCA cycle intermediate accumulation, and branched chain amino acid depletion (Kamei *et al.*, 2014). The massive oxidation of these branched amino acids may also be intended to maintain normal metabolism of cells under stressful conditions.

Oxidative stress is particularly damaging to the sulfur-containing amino acids cysteine and methionine (Ezraty *et al.*, 2017), and sulfur-containing amino acids are used as substrates for oxidative stress, thereby the concentration of cysteine was declined, and the glutathione metabolism pathway was enriched. Mitochondria use proline and arginine as metabolic fuels (Misener *et al.*, 2001). In *Bactrocera dorsalis*, gut microbiota contribute significantly to its resistance to low-temperature stress by stimulating arginine and proline metabolism (Raza *et al.*, 2020). Therefore, the lowered proline concentration was oxidized to ward off *comC* knockout stress.

CONCLUSIONS

After the knockout of *comC*, the *S. bovis* intracellular metabolites undergo dramatic changes, among which the trehalose increased by 96 times, glucose and mannitol, etc. increased by 4 times, and putrescine and 2-hydroxyglutaric acid increased by 2 times, whereas valine, leucine, isoleucine, proline and cysteine etc. were dramatically reduced. Based on the KEGG results, the metabolisms of glyoxylates and dicarboxylates, aspartates, glutamates, pyruvates, cysteines, and methionines, glutathione, and arginine were enriched. *S. bovis* promotes energy metabolism and secrets huge amounts of trehalose and mannitol to form biofilm to resists oxidative stress after *comC* knockout. The synthetic pathway of trehalose can be used as a drug target for the prevention or treatment of *S. bovis* disease.

DECLARATIONS

IRB approval

This study was approved by Animal Nutrition Institute Review Board 2023.

Supplementary material

There is supplementary material associated with this article. Access the material online at: https://dx.doi.org/10.17582/journal.pjz/20231209141813

Statement of conflict of interest

The authors have declared no conflict of interest.

REFERENCES

Ahmad, W., Mohammed, G.I., Al-Eryani, D.A., Saigl, Z.M., Alyoubi, A.O., Alwael, H. and El-Shahawi, M.S., 2020. Biogenic amines formation mechanism and determination strategies: Future challenges and limitations. *Crit. Rev. Anal. Chem.,* **50**: 485-500. https://doi.org/10.1080/10408347.2019.1657793

Amato, S.M., Orman, M.A. and Brynildsen, M.P., 2013. Metabolic control of persister formation in *Escherichia coli*. *Mol. Cell,* **50**: 475-487. https://doi.org/10.1016/j.molcel.2013.04.002

Asanuma, N., Yoshii, T., Kanada, K., Yoshizawa, K., Arai, Y., Ichikawa, T., Kawamura, A. and Hino, T., 2010. Involvement of two-component signal transduction system, *ComDE,* in the regulation of growth and genetic transformation, in the ruminal bacterium *Streptococcus bovis. Anaerobe,* **16**: 405-411. https://doi.org/10.1016/j.anaerobe.2010.05.005

Asanuma, N., Yoshii, T. and Hino, T., 2004. Molecular characterization of CcpA and involvement of this protein in transcriptional regulation of lactate dehydrogenase and pyruvate formate-lyase in the ruminal bacterium *Streptococcus bovis. Appl. environ. Microbiol.,* **70**: 5244-5251. https://doi.org/10.1128/AEM.70.9.5244-5251.2004

Câmara, A.D.A., Maréchal, P.A., Tourdot-Maréchal, R. and Husson, F., 2019. Dehydration stress responses of yeasts *Torulaspora delbrueckii, Metschnikowia pulcherrima* and *Lachancea thermotolerans*: Effects of glutathione and trehalose biosynthesis. *Fd. Microbiol.,* **79**: 137-146. https://doi.org/10.1016/j.fm.2018.12.008

Chen, W.W., Freinkman, E., Wang, T., Birsoy, K. and Sabatini, D.M., 2016. Absolute quantification of matrix metabolites reveals the dynamics of mitochondrial metabolism. *Cell*, **166**: 1324-1337. e1311. https://doi.org/10.1016/j.cell.2016.07.040

de las Rivas, B., Marcobal, A., Carrascosa, A.V. and

Muñoz, R., 2006. PCR detection of foodborne bacteria producing the biogenic amines histamine, tyramine, putrescine, and cadaverine. *J. Fd. Prot.,* **69**: 2509-2514. https://doi.org/10.4315/0362-028X-69.10.2509

Ezraty, B., Gennaris, A., Barras, F. and Collet, J.F., 2017. Oxidative stress, protein damage and repair in bacteria. *Nat. Rev. Microbiol.,* **15**: 385-396. https://doi.org/10.1038/nrmicro.2017.26

Fu, X., Chin, R.M., Vergnes, L., Hwang, H., Deng, G., Xing, Y. and Huang, J., 2015. 2-Hydroxyglutarate inhibits ATP synthase and mTOR signaling. *Cell Metab.,* **22**: 508-515. https://doi.org/10.1016/j.cmet.2015.06.009

Henao-Escobar, W., Domínguez-Renedo, O., Alonso-Lomillo, M.A. and Arcos-Martínez, M.J., 2015. Resolution of quaternary mixtures of cadaverine, histamine, putrescine and tyramine by the square wave voltammetry and partial least squares method. *Talanta,* **143**: 97-100. https://doi.org/10.1016/j.talanta.2015.05.047

Herrera, P., Kwon, Y.M. and Ricke, S.C., 2009. Ecology and pathogenicity of gastrointestinal *Streptococcus bovis. Anaerobe*, **15**: 44-54. https://doi.org/10.1016/j.anaerobe.2008.11.003

Hobley, L., Harkins, C., MacPhee, C.E. and Stanley-Wall, N.R., 2015. Giving structure to the biofilm matrix: An overview of individual strategies and emerging common themes. *FEMS Microbiol. Rev.,* **39**: 649-669. https://doi.org/10.1093/femsre/fuv015

Hu, J., Zhang, H., Zhou, S., Li, W. and He, Z.G., 2018. Characterization of a novel regulatory pathway for mannitol metabolism and its coordination with biofilm formation in *Mycobacterium smegmatis*. *J. Genet. Genom.,* **45**: 477-488. https://doi.org/10.1016/j.jgg.2018.06.007

Izanloo, H., Soleimanzadeh, A., Bucak, M.N., Imani, M. and Zhandi, M., 2021. The effects of varying concentrations of glutathione and trehalose in improving microscopic and oxidative stress parameters in Turkey semen during liquid storage at 5 °C. *Cryobiology,* **101**: 12-19. https://doi.org/10.1016/j.cryobiol.2021.07.002

Kaiki, Y., Kitagawa, H., Tadera, K., Taogoshi, H., Ikeda, M., Kano, M., Harino, T., Nomura, T., Omori, K., Shigemoto, N., Takahashi, S. and Ohge, H., 2021. Laboratory identification and clinical characteristics of *Streptococcus bovis/Streptococcus equinus* complex bacteremia: a retrospective, multicenter study in Hiroshima, Japan. *BMC Infect. Dis.,* **21**: 1192. https://doi.org/10.1186/s12879-021-06880-4

Kamei, Y., Tamada, Y., Nakayama, Y., Fukusaki, E. and Mukai, Y., 2014. Changes in transcription and metabolism during the early stage of replicative cellular senescence in budding yeast. *J. biol. Chem.,* **289**: 32081-32093. https://doi.org/10.1074/jbc.M114.600528

Koga, M., Serritella, A.V., Messmer, M.M., Hayashi-Takagi, A., Hester, L.D., Snyder, S.H. and Sedlak, T.W., 2011. Glutathione is a physiologic reservoir of neuronal glutamate. *Biochem. biophys. Res. Commun.,* **409**: 596-602. https://doi.org/10.1016/j.bbrc.2011.04.087

Kokina, A., Tanilas, K., Ozolina, Z., Pleiko, K., Shvirksts, K., Vamza, I. and Liepins, J., 2022. Purine auxotrophic starvation evokes phenotype similar to stationary phase cells in budding yeast. *J. Fungi,* **8**: 29. https://doi.org/10.3390/jof8010029

Misener, S.R., Chen, C.P. and Walker, V.K., 2001. Cold tolerance and proline metabolic gene expression in *Drosophila melanogaster. J. Insect Physiol.,* **47**: 393-400. https://doi.org/10.1016/S0022-1910(00)00141-4

OmerOglou, E., Karaca, B., Kibar, H., Haliscelik, O. and Kiran, F., 2022. The role of microbiota-derived postbiotic mediators on biofilm formation and quorum sensing-mediated virulence of *Streptococcus mutans*: A perspective on preventing dental caries. *Microb. Pathog.,* **164**:105390. https://doi.org/ 10.1016/j.micpath.2022.105390

Öberg, J. and Nilson, B., 2022. Bacteraemia and infective endocarditis with *Streptococcus bovis-Streptococcus equinus*-complex: A retrospective cohort study. *Infect. Dis.* (Lond.), **54**: 760-765. https://doi.org/10.1080/23744235.2022.2089730

Padilla-Guerrero, I.E., Barelli, L., González-Hernández, G.A., Torres-Guzmán, J.C. and Bidochka, M.J., 2011. Flexible metabolism in *Metarhizium anisopliae* and *Beauveria bassiana*: Role of the glyoxylate cycle during insect pathogenesis. *Microbiology* (Reading), **157**: 199-208. https://doi.org/10.1099/mic.0.042697-0

Peterson, B.W., He, Y., Ren, Y., Zerdoum, A., Libera, M.R., Sharma, P.K. and Busscher, H.J., 2015. Viscoelasticity of biofilms and their recalcitrance to mechanical and chemical challenges. *FEMS Microbiol. Rev.,* **39**: 234-245. https://doi.org/10.1093/femsre/fuu008

Pompilio, A., Bonaventura, G.D. and Gherardi, G., 2019. An overview on *Streptococcus bovis/Streptococcus equinus* complex isolates: Identification to the species/subspecies level and antibiotic resistance. *Int. J. Mol. Sci.,* **20**: 480. https://doi.org/10.3390/

ijms20030480

Qiu, S., Xu, Y., Huang, L., Zheng, W., Huang, C., Huang, S. and Pan, J., 2016. Non-invasive detection of nasopharyngeal carcinoma using saliva surface-enhanced Raman spectroscopy. *Oncol. Lett.,* **11**: 884-890. https://doi.org/10.3892/ol.2015.3969

Raza, M.F., Wang, Y., Cai, Z., Bai, S., Yao, Z., Awan, U.A. and Zhang, H., 2020. Gut microbiota promotes host resistance to low-temperature stress by stimulating its arginine and proline metabolism pathway in adult *Bactrocera dorsalis. PLOS Pathog*., **16**: e1008441. https://doi.org/10.1371/journal.ppat.1008441

Senpuku, H., Mohri, S., Mihara, M., Arai, T., Suzuki, Y. and Saeki, Y., 2019. Effects of 7S globulin 3 derived from the adzuki bean [Vigna angularis] on the CSP- and eDNA- dependent biofilm formation of *Streptococcus mutans. Arch. Oral Biol.,* **102**: 256-265. https://doi.org/10.1016/j.archoralbio.2019.04.010

Shao, Y., Li, C., Chen, X., Zhang, P., Li, Y., Li, T. and Jiang, J., 2015. Metabolomic responses of sea cucumber *Apostichopus japonicus* to thermal stresses. *Aquaculture,* **435**: 390-397. https://doi.org/10.1016/j.aquaculture.2014.10.023

Shui, Y., Jiang, Q., Lyu, X., Wang, L., lin, Y., Ma, Q., Gong, T., Zeng, J., Yang, R. and Li, Y., 2021. Inhibitory effects of sodium new houttuyfonate on growth and biofilm formation of *Streptococcus mutans. Microb. Pathog.,* **157**:104957. https://doi.org/ 10.1016/j.micpath.2021.104957

Smart, K.F., Aggio, R.B., Van Houtte, J.R. and Villas-Bôas, S.G., 2010. Analytical platform for metabolome analysis of microbial cells using methyl chloroformate derivatization followed by gas chromatography-mass spectrometry. *Nat. Protoc.,* **5**: 1709-1729. https://doi.org/10.1038/nprot.2010.108

Suntharalingam, P. and Cvitkovitch, D.G., 2005. Quorum sensing in streptococcal biofilm formation. *Trends Microbiol.,* **13**: 3-6. https://doi.org/10.1016/j.tim.2004.11.009

Suzuki, Y., Nagasawa, R. and Senpuku, H., 2017. Inhibiting effects of fructanase on competence-stimulating peptide-dependent quorum sensing system in *Streptococcus mutans. J. Infect. Chemother.,* **23**: 634-641. https://doi.org/10.1016/j.jiac.2017.06.006

Wei, Y., Yan, Z., Liu, M., Chen, D., Chen, X. and Li, X., 2022. Metabolic characteristics of intracellular trehalose enrichment in salt-tolerant *Zygosaccharomyces rouxii. Front. Microbiol.,* **13**: 935756. https://doi.org/10.3389/fmicb.2022.935756

Yang, Y. and Tal-Gan, Y., 2019. Exploring the competence stimulating peptide (CSP) N-terminal requirements for effective ComD receptor activation in group1 *Streptococcus pneumoniae. Bioorg. Chem.,* **89**: 102987. https://doi.org/10.1016/j.bioorg.2019.102987.

Supplementary Material

Streptococcus bovis JB1 Protects Against Oxidative Stress Caused by *comC* Knockout by Increasing Trehalose Secretion

Quanhui Peng[1]*, Ali Mujtaba Shah[2]*, Wang Zhi-Sheng[1], Xue Bai[1], Wang Li-Zhi[1], Zou Hua-Wei[1], Ali Raza Shah[3], Jiang Ya-Hui[1], Hu Rui[1] and Xiao Jian-Xing[1]

[1]*Institute of Animal Nutrition, Key Laboratory of Bovine Low-Carbon Farming and Safe Production, Sichuan Agricultural University, Chengdu, 611130, PR China*
[2]*Key Laboratory of Animal Genetics, Breeding and Reproduction of Shaanxi Province, College of Animal Science and Technology, Northwest A and F University, Yangling 712100, China.*
[3]*Khairpur College of Agricultural Engineering and Technology, Sindh Agriculture University, Tandojam, 66000, Sindh, Pakistan*

Quanhui Peng and Ali Mujtaba Shah contributed equally to this work.

Supplementary Table S1. Composition and nutrient level of diet (Dry matter basis, %).

| Ingredients	Ratio	[2]Nutrient level	
Corn	18.75	ME (MJ/kg)	7.55
Wheat bran	6.00	CP	12.61
Soybean meal	1.50	NDF	38.95
Rapeseed meal	2.70	ADF	28.84
Rice straw	40.00	Ca	0.60
Distilled grain	30.00	TP	0.33
CaCO$_3$	0.45		
NaHCO$_3$	0.15		
NaCl	0.15		
[1]Premix	0.30		

[1]One kilogram of premix contained: VA 1100000 IU, VD$_3$ 440000 IU, VE 3300 IU, Fe 16.67 g, Cu 3.33 g, Mn 6.67 g, Zn 10 g, I 170 mg, Se 70 mg, Co 30 mg. [2]ME was calculated, while the other nutrient levels were measured.

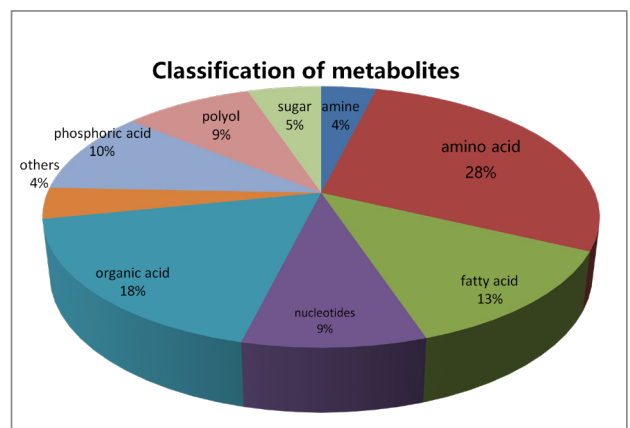* Corresponding author: pengquanhui@126.com, alimujtabashah@nwafu.edu.cn
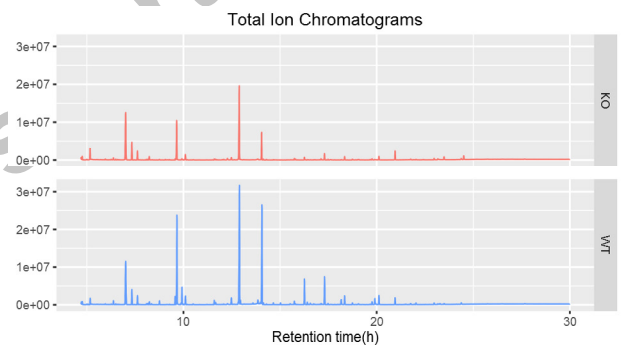
Supplementary Fig. S1. Representative spectra of intracellular content obtained from *Sreptococcus bovis* JB1 wild type and *ΔcomC* mutant.

Supplementary Fig. 2S. Classification of 78 annotated metabolites obtained from intracellular of *Sreptococcus bovis* JB1 wild type and *ΔcomC* mutant.